NEOPLASIA
www.neoplasia.com

Volume 13 Number 3 March 2011 pp. 217–229 217

Irinotecan Synergistically Enhances the Antiproliferative and Proapoptotic Effects of Axitinib *In Vitro* and Improves Its Anticancer Activity *In Vivo*[1]

Bastianina Canu[*,†], Anna Fioravanti[*,†], Paola Orlandi[*,†], Teresa Di Desidero[*,†], Greta Alì[‡], Gabriella Fontanini[‡], Antonello Di Paolo[*], Mario Del Tacca[§], Romano Danesi[*] and Guido Bocci[*,†]

[*]Division of Pharmacology, Department of Internal Medicine, University of Pisa, Pisa, Italy; [†]Istituto Toscano Tumori, Italy; [‡]Division of Pathological Anatomy, Department of Surgery, University of Pisa, Pisa, Italy; [§]Clinical Pharmacology Centre for Drug Experimentation, University of Pisa, Pisa, Italy

Abstract

AIMS: To demonstrate the synergistic antiproliferative and proapoptotic activity of irinotecan and axitinib *in vitro* and the improvement of the *in vivo* effects on angiogenesis and pancreatic cancer. *METHODS:* Proliferation and apoptotic assays were performed on human dermal microvascular endothelial cells and pancreas cancer (MIAPaCa-2, Capan-1) cell lines exposed to SN-38, the active metabolite of irinotecan, axitinib, or their simultaneous combination for 72 hours. ERK1/2 and Akt phosphorylation, the vascular endothelial growth factor (VEGF), VEGF receptor-2, and thrombospondin-1 (TSP-1) concentration were measured by ELISAs. *ATP7A* and *ABCG2* gene expression was performed with real-time polymerase chain reaction and SN-38 intracellular concentrations were measured by high-performance liquid chromatography. Capan-1 xenografts in nude mice were treated with irinotecan and axitinib alone or in simultaneous combination. *RESULTS:* A strong synergistic effect on antiproliferative and proapoptotic activity was found with the axitinib/SN-38 combination on endothelial and cancer cells. ERK1/2 and Akt phosphorylation were significantly inhibited by lower concentrations of the combined drugs in all the cell lines. Axitinib and SN-38 combined treatment greatly inhibited the expression of the *ATP7A* and *ABCG2* genes in endothelial and cancer cells, increasing the SN-38 intracellular concentration. Moreover, TSP-1 secretion was increased in cells treated with both drugs, whereas VEGFR-2 levels significantly decreased. *In vivo* administration of the simultaneous combination determined an almost complete regression of tumors and tumor neovascularization. *CONCLUSIONS: In vitro* results show the highly synergistic properties of simultaneous combination of irinotecan and axitinib on endothelial and pancreas cancer cells, suggesting a possible translation of this schedule into the clinics.

Neoplasia (2011) 13, 217–229

Abbreviations: ATP7A, copper-transporting P-type ATPase; ABCG2, ATP-binding cassette subfamily G member 2; CI, combination index; DRI, dose reduction index; HMVEC-d, human dermal microvascular endothelial cells; MTD, maximum tolerated dose; TSP-1, thrombospondin-1; VEGF, vascular endothelial growth factor; VEGFR-2, vascular endothelial growth factor receptor-2

Address all correspondence to: Guido Bocci, MD, PhD, Division of Pharmacology, Department of Internal Medicine, University of Pisa & Istituto Toscano Tumori, Via Roma, 55, I-56126 Pisa, Italy. E-mail: g.bocci@med.unipi.it

[1]This article refers to supplementary materials, which are designated by Figures W1 and W2 and are available online at www.neoplasia.com.

Received 13 September 2010; Revised 22 November 2010; Accepted 29 November 2010

DOI 10.1593/neo.101334

Introduction

Axitinib (AG-013736), a novel multitarget tyrosine kinase inhibitor, has been recently introduced in clinical trials, often in combination with chemotherapeutic drugs [1] as a potent, oral antiangiogenic drug, mainly targeting the vascular endothelial growth factor receptor-2 (VEGFR-2) tyrosine kinase domain [2–4]. A number of preclinical studies have been published on this compound, showing an *in vivo* antitumor activity in breast [5], prostate [6–8], exocrine and endocrine pancreas [4,9], colon, renal cell, and ovarian cancer [4]. The *in vivo* antitumor effects were mainly due to the antiangiogenic property of the molecule as demonstrated by immunohistochemistry (IHC) [5,9] and dynamic contrast-enhanced magnetic resonance imaging [5]. Some combination therapies has been tested *in vivo* to increase the antitumor activity of the compound. Metronomic and standard doses of cyclophosphamide [6,10], gemcitabine, docetaxel, and carboplatin [4] have been successfully used *in vivo* in human pancreas, breast, and ovarian cancer xenografts.

Pancreatic cancer is a leading cause of tumor deaths among oncologic diseases. The 5-year survival in early diagnosed and surgically treated patients ranges from 12% to 20% [11]. Metastatic pancreatic cancer remains resistant to current chemotherapy and radiotherapy. Although gemcitabine is the main used drug for systemic treatment of pancreatic cancer patients, it does not significantly prolong the survival of the patients. Alternative therapeutic options are urgently needed to improve the tumor response and survival. For these reasons, numerous combinations have been assessed in preclinical studies, usually using gemcitabine combined with various drugs such as fluvastatin [12] and antiangiogenic agents [13–15]. Irinotecan (CPT-11) is a standard therapeutic choice for colorectal cancer, but few phase 1 to 2 clinical studies, combining gemcitabine with irinotecan [16,17], to treat pancreatic cancer have been undertaken; moreover, a few preclinical studies assessing single drug administration [18,19] or its combination with GEM231, a second-generation antisense oligonucleotide [20] or TRA-8, an agonistic antibody to death receptor 5 [21], have been recently assessed in pancreas cancer.

Cellular drug resistance is a major obstacle in pancreas cancer therapy. Cancer cells can be intrinsically resistant or acquire resistance to both cytotoxic and novel molecularly targeted drugs. This form of multidrug resistance can be conveyed by several mechanisms including the active ATP-dependent transport of drugs out of the cell by efflux pumps belonging to the ATP-binding cassette (ABC) family of transporters [22]. ABCG2 overexpression has been associated with a marked decrease in the intracellular accumulation of SN-38, the active metabolite of irinotecan, and with the highest resistance level of colorectal and endometrial cancer cells, confirming that ABCG2 is directly involved in acquired resistance to SN-38 [23,24]. Moreover, the copper-transporting P-type ATPase ATP7A has been recently implicated in multidrug resistance to chemotherapy by enhancing efflux of drugs such as cisplatin, paclitaxel, doxorubicin, and SN-38 [25,26]. These findings strongly suggest that both ABCG2 and ATP7A expression could modulate the efflux rates of SN-38 from cancer cells.

Thus, our approach to combination therapy studies in pancreas cancer involves both irinotecan and axitinib to answer to the open issue about tumor responsiveness. The purposes of our study were 1) to demonstrate the synergistic interaction *in vitro* between SN-38 and axitinib in endothelial/pancreas cancer cells and an improvement of anticancer activity *in vivo* by the simultaneous combination of irinotecan and axitinib and 2) to elucidate the molecular mechanisms of the antiproliferative and proapoptotic activities that may be mediated by this particular combination treatment.

Materials and Methods

In Vitro *Studies*

Materials, drugs, and cells lines. Recombinant human vascular endothelial growth factor (rhVEGF) and recombinant human epidermal growth factor (rhEGF) were from PeproTechEC Ltd (London, UK). Cell culture media MCDB131, RPMI, and Dulbecco modified Eagle medium; fetal bovine serum (FBS); horse serum (HS); L-glutamine; penicillin; streptomycin; and antibiotics were from Gibco (Gaithersburg, MD). Type A gelatin from porcine skin, supplements, and all other chemicals not listed in this section were obtained from Sigma Chemical Co (St Louis, MO). Plastics for cell culture were supplied by Costar (Cambridge, MA).

Axitinib and irinotecan and its active metabolite SN-38 were kindly provided by Pfizer (Groton, MD). For the *in vitro* experiments, the drugs were dissolved in DMSO and diluted as needed; for the *in vivo* studies, irinotecan was diluted in saline and administered intraperitoneally (i.p.), whereas axitinib was formulated in 0.5% carboxymethylcellulose/H_2O·HCl (g/v, pH 2-3) and dosed as a suspension at 5 ml/kg orally twice daily [4].

The human dermal microvascular endothelial cells (HMVEC-d; Clonetics, San Diego, CA) were maintained in MCDB131 culture medium supplemented with antibiotics, 10% heat-inactivated FBS, L-glutamine (2 mM), heparin (10 IU/ml), rhEGF (10 ng/ml), and basic fibroblast growth factor (5 ng/ml). The human pancreatic cancer cell line MIAPaCa-2 was obtained from the American Type Culture Collection (ATCC, Manassas, VA), maintained in Dulbecco modified Eagle medium, and supplemented with 10% FBS, 2.5% HS, antibiotics and L-glutamine. The human pancreatic cancer cell line Capan-1 was obtained from the ATCC, maintained in RPMI medium, and supplemented with 15% FBS, L-glutamine, and antibiotics.

Cell proliferation assay. HMVEC-d (6×10^4 cells/well), Capan-1 (2×10^4 cells/well), and MIAPaCa-2 (2×10^4 cells/well) cells were plated in 24-well plates (1% gelatin-coated for HMVEC-d) and allowed to attach overnight. Endothelial cells were treated with axitinib (0.01-1000 nM) and SN-38 (0.001-1000 nM) or with their vehicles continuously for 72 hours in 1 ml of medium, adding fresh medium with drugs every 24 hours. In separate experiments, tumor cell lines were treated with axitinib (0.001-100 μM) and SN-38 (0.001-100 μM) or with their vehicles for 72 hours. At the end of the treatment, the cells were harvested with trypsin/EDTA, and the viable cells were counted with a hemocytometer; the growth of treated cells was expressed as a percentage of control cultures (vehicle alone). The concentration of drugs that decreased cell count by 50% (IC_{50}) compared with controls was calculated by nonlinear fitting of experimental data. All experiments were repeated, independently, three times with at least nine samples for each concentration.

In vitro *assessment of synergism between axitinib and SN-38 on endothelial and tumor cells.* The combination of SN-38 and axitinib was explored with the treatment schedule at a *simultaneous exposure* with a fixed molar concentration ratio of 1:1 on HMVEC-d and MIAPaCa-2 cells or 1:10 on Capan-1 cells for 72 hours. To evaluate the level of interaction (synergistic, additive, or antagonistic)

between SN-38 and axitinib, the method proposed by Chou [27] was followed. Briefly, synergism or antagonism for axitinib plus SN-38 was calculated on the basis of the multiple drug-effect equation and quantified by the combination index (CI), where CI < 1, CI = 1, and CI > 1 indicate synergism, additive effect, and antagonism, respectively. On the basis of the classic isobologram for mutually exclusive effects, the CI value was calculated as follows:

$$CI = [(D)_1 / (D_x)_1] + [(D)_2 / (D_x)_2]$$

As an example, at the 50% inhibition level, $(D_x)_1$ and $(D_x)_2$ are the concentrations of axitinib and SN-38, respectively, that induce a 50% inhibition of cell growth; $(D)_1$ and $(D)_2$ are the concentrations of axitinib and SN-38 in combination that also inhibits cell growth by 50% (isoeffective as compared with the single drugs alone). The dose reduction index (DRI) defined the degree of dose reduction that is possible in a combination for a given degree of effect as compared with the concentration of each drug alone:

$$(DRI)_1 = (D_x)_1 / (D)_1 \text{ and } (DRI)_2 = (D_x)_2 / (D)_2$$

The CI and DRI indexes were calculated with the CalcuSyn v.2.0 software (Biosoft, Cambridge, UK).

Apoptosis measurements. To quantify the apoptotic process, endothelial and cancer cells were treated for 72 hours with axitinib (0.01-1000 nM), SN-38 (0.01-1000 nM), and the simultaneous axitinib/SN-38 combination and vehicle alone. At the end of the experiment, cells were collected and the Cell Death Detection ELISA Plus kit (F. Hoffmann-La Roche Ltd, Basel, Switzerland) was used. All the absorbance values were plotted as a percentage of apoptosis relative to control cells (vehicle only), labeled as 100%. All experiments were repeated three times with at least three replicates per sample.

ERK1/2 (pTpY185/187) and Akt ($pThr^{308}$) ELISA assay. To detect the phosphorylation of ERK1/2 and Akt in endothelial and cancer cells after a 72-hour drug treatment, cells were exposed to axitinib, SN-38, and their simultaneous combination (1:1 or 1:10 fixed molar concentration) at concentrations corresponding to the experimental IC_{50} of cell proliferation or with vehicle alone for 72 hours. To measure pERK1/2 and pAkt, at the end of the experiment, the cells were harvested and immediately frozen with liquid nitrogen. Cells were lysed as per manufacturer's instructions. Each sample was then assayed for human ERK1/2 and Akt phosphorylation by the PhosphoDetect ERK1/2 ($pThr^{185}$/$pTyr^{187}$) ELISA Kit and the PhosphoDetect Akt ($pThr^{308}$) ELISA Kit (Calbiochem, Darmstadt, Germany) and normalized by total protein ERK1/2 and Akt concentration, respectively. The optical density was determined using the microplate reader Multiskan Spectrum (Thermo Labsystems, Milan, Italy) set to 450 nm. The results were expressed as percentage of pERK1/2 and pAKT of controls. All experiments were repeated, independently, six times with at least nine samples for each concentration.

Real-time polymerase chain reaction analysis of ATP7A *and* ABCG2 *gene expression on tumor and endothelial cells.* To evaluate the expression of the human *ATP7A* and *ABCG2* genes, 6×10^4 HMVEC-d, 2×10^4 MIAPaCa-2 and Capan-1 cells were grown in their respective media and treated with axitinib, SN-38, and their simultaneous combination at a concentration corresponding to the experimental IC_{50} of cell proliferation and at higher and lower doses or with vehicle alone for 72 hours. Briefly, RNA (1 μg) was reverse transcribed as previously described [28], and the resulting complementary DNA was diluted (2:3) and then amplified by quantitative reverse transcription–polymerase chain reaction with a sequence detection system (7900HT; Applied Biosystems, Carlsbad, CA). *ATP7A*- and *ABCG2*-validated primers were purchased from Applied Biosystems (Assay ID Hs00921967_m1 and Hs01053796_m1, respectively). The polymerase chain reaction thermal cycling conditions and optimization of primer concentrations were followed as per manufacturer's instructions. Amplifications were normalized to glyceraldehyde 3-phosphate dehydrogenase (*GAPDH*), and the quantitation of gene expression was performed using the $\Delta\Delta C_t$ calculation, where C_t is the threshold cycle; the amount of target, normalized to the endogenous control and relative to the calibrator (vehicle-treated control cells), is given as $2^{-\Delta\Delta C_t}$. All experiments were repeated, independently, three times with at least nine samples for each concentration.

High-performance liquid chromatography analysis of SN-38 concentrations in endothelial cells. The quantitative analysis of irinotecan's main metabolite SN-38 in cells was performed as previously described [29] with minor modifications. Endothelial cells were treated with vehicle alone, SN-38 (1 μM), axitinib (1 μM), or a combination of the two (SN-38 1 μM + axitinib 1 μM) for 72 hours. At the end of the experiment, the cells were collected, counted to obtain the same number of cells in each sample (10^5 cells), and centrifuged. The cells were frozen and thawed three times consecutively. Briefly, concentrations of SN-38 were evaluated after extracting with methanol containing 0.1% HCl 10 N. The samples were then centrifuged, and the clear supernatant was evaporated to dryness under nitrogen flow in a thermostated bath at 45°C. The resulting pellet was reconstituted in methanol acidified with 0.1% HCl 10 N and eluted through a μBondapack C18 stationary phase column (300 × 3.9 mm, 10 μm; Waters, Milford, MA) by KH_2PO_4 0.1 M/acetonitrile (60:40, vol/vol; pH 6.0) containing 3 mM sodium heptanesulfonate. The chromatographic system LC Module I Plus (Waters) was equipped with a Model 474 scanning fluorescence detector with excitation and emission wavelengths set at 375 and 525 nm, respectively. Data analysis was performed using Millennium 2.1 software (Waters). Standard calibration curves were generated by adding SN-38 to 1 ml of PBS, resulting in final concentrations that ranged from 2500 to 0.16 ng/ml. The range of linearity of the high-performance liquid chromatography method was from 2500 to 0.16 ng/ml.

VEGF, thrombospondin-1, and VEGFR-2 detection in conditioned media and cell lysate by ELISA. HMVEC-d, Capan-1, and MIAPaCa-2 cells were grown in their respective media and treated with SN-38 and axitinib at a concentration corresponding to the experimental IC_{50} of cell proliferation and at higher and lower concentrations or using simultaneous combination treatment. To measure secreted VEGF and thrombospondin-1 (TSP-1), at the end of the experiment, the medium of each well was discarded and replaced with serum-free medium for 4 hours. Each sample was then assayed for human VEGF and TSP-1 concentrations by the VEGF and TSP-1 ELISA Kit Quantikine (R&D System, Minneapolis, MN), respectively, and normalized by total protein concentration. The sVEGFR-2 ELISA Kit Quantikine (R&D Systems) was used to measure VEGFR-2 protein concentrations in the endothelial cell lysate; the results were normalized

per number of cells. The optical density was determined using the microplate reader Multiskan Spectrum set to 450 nm (with a wavelength correction set to 540 nm). All experiments were repeated, independently, three times with at least nine samples for each concentration.

In Vivo *Studies*

Animals and treatments. The CD *nu/nu* male mice, weighing 20 g, were supplied by Charles River (Milan, Italy) and were allowed unrestricted access to sterile food and tap water. Housing and all procedures involving animals were performed according to the protocol approved (approval no. 2741) by the *Comitato di Ateneo per la sperimentazione animale* (Academic Committee for the animal experimentation) of the University of Pisa, in accordance with the European Community Council Directive 86-609, recognized by the Italian government, on animal welfare. Each experiment used the minimum number of mice needed to obtain statistically meaningful results.

On day 0, $2 \times 10^6 \pm 5\%$ viable Capan-1 cells/mouse were inoculated subcutaneously. Animal weights were monitored, and on appearance of a subcutaneous mass, tumor dimensions were measured every 2 days using calipers. Tumor volume (mm^3) was defined as follows: $[(w_1 \times w_1 \times w_2) \times (\pi/6)]$, where w_1 and w_2 were the largest and the smallest tumor diameter (mm), respectively. The mice were randomized into groups of six animals. Treatment was delivered once the tumor reached ~100 mm^3, from day 8 to 10 after cell inoculation. Axitinib, irinotecan, or their simultaneous combination was administered as follows: 1) axitinib 25 mg/kg per os (p.o.) twice a day for 31 days, 2) irinotecan 100 mg/kg weekly for 4 weeks, 3) simultaneous combination of axitinib and irinotecan at each of the above schedules. Mice from the control group were injected i.p. with saline and p.o. with vehicle alone. The experimental period ended 7 days after the last administration of axitinib. Mice were killed by an anesthetic overdose, and tumors were excised, measured, and sampled for IHC. Drug efficacy was based on percentage of the average treated tumor volume divided by the average vehicle control tumor volume (% *T*/*C*) [28].

Immunohistochemistry. Briefly, tumor tissue samples from all the different treatment groups were fixed in 10% neutral-buffered formalin for 12 to 24 hours and embedded in paraffin for histology and IHC. Sections of the tumor (5 μm thick) were stained with hematoxylin and eosin. Immunostainings were performed by a Benchmark immunostainer (Ventana, Tucson, AZ) using the avidin-biotin-peroxidase complex (ABC) method and counterstained with hematoxylin. Negative controls were carried out by omitting the primary antibodies. IHC evaluated independently by two pathologists (G.A. and G.F.) blinded to the treatment code.

Microvascular count was determined using anti-FVIII polyclonal antibody (Ventana Medical System). A single microvessel was defined as any immunostained endothelial cell separated from adjacent microvessel, tumor cells, and other connective tissue elements. Samples were examined by each pathologist, who identified the area with most intense vascularization (hot spot) under low microscopic power (×100). A region of 0.74 mm^2/field was then scanned at ×250 microscope magnification. Five fields were analyzed, and for each of them, the number of stained blood vessels was counted. For individual tumors, microvascular count was scored by averaging the five field counts. Large vessels with thick, muscular walls were excluded from the counts. The presence of a lumen was not required for scoring as a microvessel.

IHC detection of apoptosis-related protein was carried out using a rabbit polyclonal antibody to active caspase-3 (diluted 1:2000; Abcam, Cambridge, UK) that specifically recognizes the large fragment (17 kDa) of the active protein but not full-length caspase-3. The antibody selectively stained the cytoplasm of apoptotic cells. The apoptotic index (AI) was obtained by examination of the sections stained using IHC and all the identifiable cells exhibiting staining were counted. Apoptotic cells, which were present in areas where intense necrosis had occurred, were excluded from analysis. AI was calculated as a percentage of the apoptotic cells out of the total number of the examined cells [30,31].

Statistical analysis. The analysis by analysis of variance, followed by the Student-Newman-Keuls test, was used to assess the statistical differences of data *in vitro* and *in vivo*. $P < .05$ was considered significant. Statistical analyses were performed using the GraphPad Prism software package version 5.0 (GraphPad Software, Inc, San Diego, CA).

Results

Axitinib and SN-38 Inhibit Endothelial and Cancer Cell Proliferation In Vitro

In vitro axitinib and SN-38 inhibited the cell proliferation of HMVEC-d and of the pancreatic cancer cell line Capan-1 and MIAPaCa-2 in a concentration-dependent manner (Figure 1); the 72-hour axitinib exposure inhibited the proliferation of HMVEC-d with an IC_{50} of 30.5 ± 12.9 nM (Figure 1*A*), being significantly different from those observed in MIAPaCa-2 and Capan-1 (0.80 ± 0.35 and 0.84 ± 0.34 μM, respectively; Figure 1, *B* and *C*). In contrast, a greater antiproliferative effect of SN-38 on Capan-1 and MIAPaCa-2 was found as demonstrated by the IC_{50} values (0.040 ± 0.032 and 0.29 ± 0.023 μM, respectively; Figure 1, *B* and *C*). The cytotoxic activity on proliferating HMVEC-d was similar to the one observed with axitinib (IC_{50}, 13.3 ± 4.7 nM; Figure 1*A*).

Synergistic Effect of Axitinib and SN-38 on HMVEC-d, Capan-1, and MIAPaCa-2 Cell Proliferation

Simultaneous and continuous exposure of HMVEC-d, MIAPaCa-2, and Capan-1 cells to different concentrations of SN-38 and axitinib for 72 hours showed a strong synergism (CI < 1 and DRI > 1; Table 1). Synergism corresponding to CI < 1 always yielded a favorable DRI > 1 for both drugs (Table 1). The CI and DRI values at IC_{25}, IC_{50}, and IC_{75} are reported in Table 1. Figure 1*D* shows a representative isobologram of HMVEC-d cells exposed to axitinib and SN-38 for 72 hours with the simultaneous schedule of treatment. Furthermore, the simultaneous treatments of axitinib and SN-38 for 72 hours were synergistically active on pancreatic Capan-1 and MIAPaCa-2 cell proliferation, as shown by the representative isobolograms in Figure 1, *E* and *F*, respectively. The position of the data points on the left of the line connecting the IC_{50} and IC_{90} values of axitinib and SN-38 indicates synergism for the schedule (Figure 1, *D-F*).

Induction of Apoptosis by Axitinib, SN-38, and Their Combination

The extent of DNA fragmentation was dependent on the concentration of both drugs. In particular, the presence of chromatin fragments was clearly detectable after 72 hours in a dose-dependent manner for axitinib and SN-38, alone and simultaneously combined

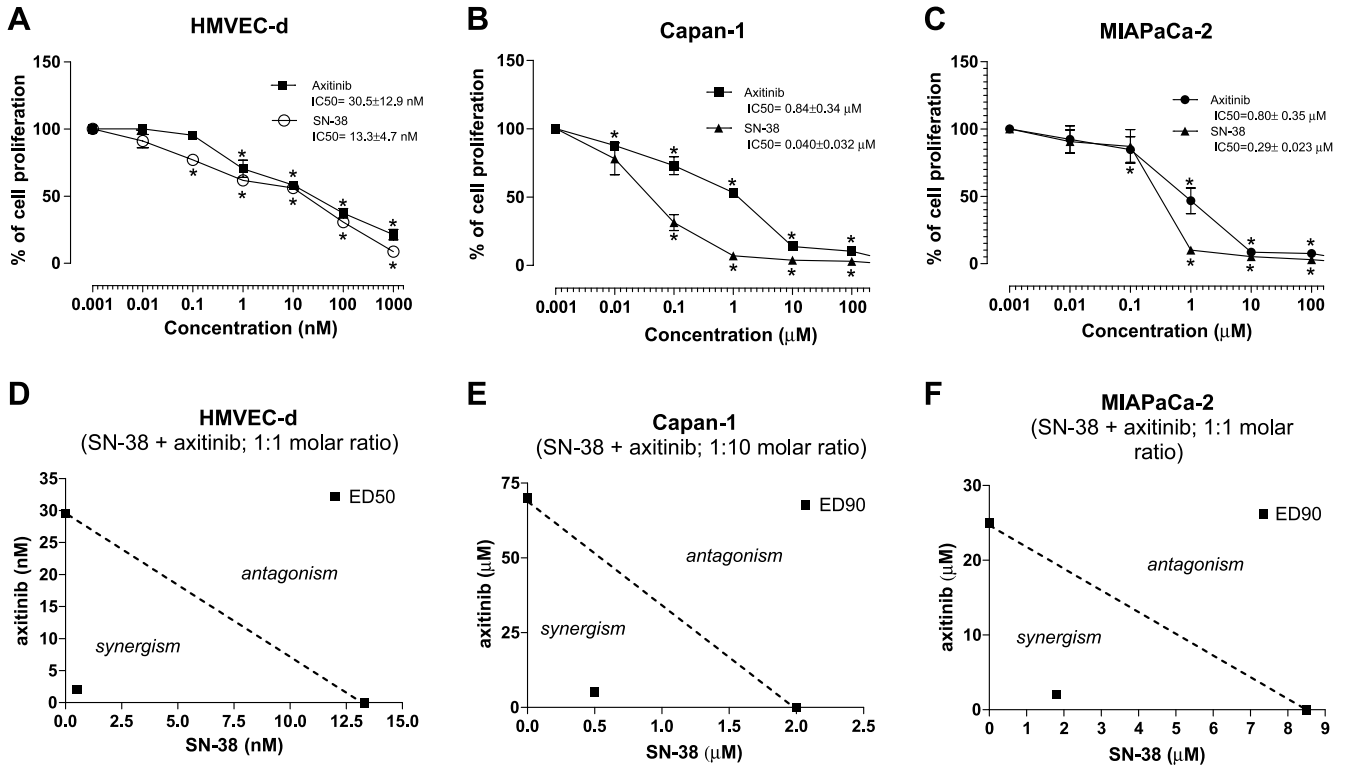

Figure 1. Effect of axitinib and SN-38, the active metabolite of irinotecan, on *in vitro* cell proliferation (A-C). The antiproliferative effects of the drugs were studied using continuous exposures (72 hours) on HMVEC-d (A), Capan-1 (B), and MIAPaCa-2 cell lines (C). Symbols and bars indicate mean values ± SE, respectively. *$P < .05$ *versus* vehicle-treated controls. IC_{50} indicates the concentration of drug that reduced cell proliferation by 50%. Isobologram analyses of HMVEC-d (D), Capan-1 (E), and MIAPaCa-2 (F) cell proliferation inhibition by simultaneous combination of axitinib and SN-38. The IC_{50} and IC_{90} values of each drug are plotted on the axes; the solid line represents the addictive effect, whereas the point representing the concentrations of axitinib and SN-38 resulting in 50% or 90% proliferation inhibition of the combination is reported on the left of the connecting line, indicating synergism.

(Figure 2). As shown in the upper part of Figure 2*A*, after 72 hours of treatment with axitinib and SN-38, a significant percentage of apoptotic endothelial cells in the treated samples were found when compared to controls. These percentages were similar to those obtained when cells were treated at much lower concentrations in the simultaneous axitinib/SN-38 combination (Figure 2*A*, *lower part*). Furthermore, the same proapoptotic effects of axitinib and SN-38, alone and in combination, were observed also in both cancer cell lines Capan-1 and MIAPaCa-2 (Figure 2, *B* and *C*, respectively).

Table 1. CI and DRI Values for the Drug Combinations at 25%, 50%, and 75% Levels of Inhibition of HMVEC-d, Capan-1, and MIAPaCa-2 Cell Proliferation.

Cells	CI Values		
	25% (Axitinib +SN-38)	50% (Axitinib + SN-38)	75% (Axitinib + SN-38)
HMVEC-d	0.008	0.082	0.877
Capan-1	1.074	0.711	0.473
MIAPaCa-2	0.219	0.173	0.173

Cells	DRI Values					
	25%		50%		75%	
	Axitinib	SN-38	Axitinib	SN-38	Axitinib	SN-38
HMVEC-d	>500	144.228	75.497	14.447	5.368	1.447
Capan-1	2.891	1.373	4.898	1.974	8.298	2.837
MIAPaCa-2	4.930	62.436	7.283	27.887	10.760	12.456

Inhibition of ERK1/2 and Akt Phosphorylation in Endothelial and Cancer Cells by the Drug Combination

After exposure to SN-38, axitinib, and their simultaneous combination at the concentration corresponding to experimental IC_{50} of cell proliferation reduced the amount of the active, phosphorylated form of ERK1/2 and Akt in HMVEC-d cells (Figure 3*A*). The ratio of phosphorylated/nonphosphorylated ERK1/2 and Akt proteins of treated cells seemed significantly decreased also in Capan-1 and MIAPaCa-2 cells, respectively (Figure 3, *B* and *C*). Interestingly, the combination of the two drugs synergistically enhanced the inhibition of phosphorylation of both ERK1/2 and Akt in all the tested cell lines; indeed, much lower concentrations of the combined drugs obtained similar inhibitory effects of the single drug schedules.

Combination of Axitinib and SN-38 Inhibits ABCG2 *and* ATP7A *Gene Expression in Endothelial and Cancer Cells*

To study the effect of the combination treatment to the variation of *ATP7A* and *ABCG2* expression, the gene expression of these transporters was quantified in all the three cell lines exposed to different drug concentrations. Figure 4, *A* and *B*, showed the concentration-dependent and significant inhibition of the gene expression of *ATP7A* and *ABCG2* in Capan-1 and MIAPaCa-2 cells, respectively, by

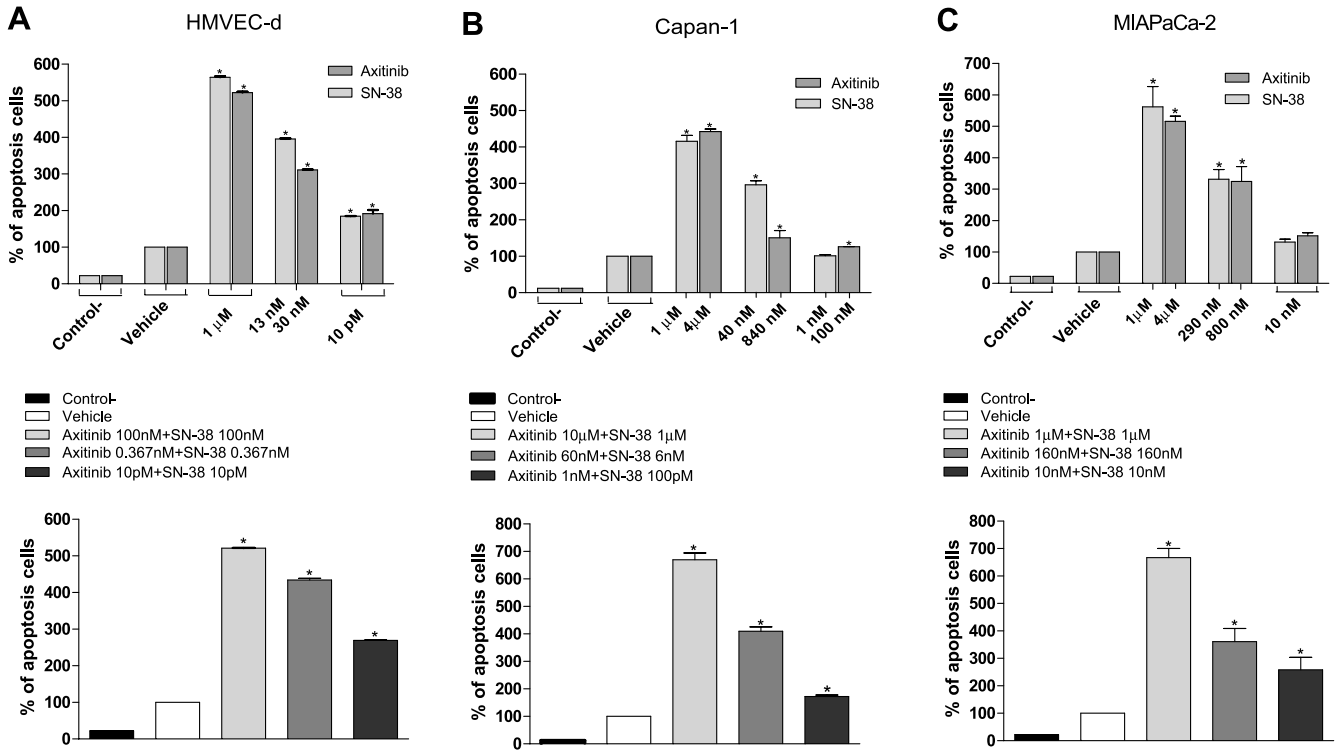

Figure 2. Proapoptotic effects of SN-38 and axitinib on proliferating HMVEC-d (A, upper part), Capan-1 (B, upper part), and MIAPaCa-2 (C, upper part) cells treated for 72 hours. The enhanced proapoptotic effects of the combined treatment was determined on HMVEC-d (A, lower part), Capan-1 (B, lower part) and MIAPaCa-2 (C, lower part) cells. Columns and bars indicate mean values ± SE, respectively. *$P < .05$ *versus* vehicle-treated controls. Control− stands for the negative control of the ELISA kit.

axitinib, SN-38, and their simultaneous combination. Moreover, in HMVEC-d cells, the combination of the two drugs caused significant decreases in the expression of *ATP7A* and *ABCG2* at much lower concentrations of the two drugs (Figure 4*C*).

On the basis of these findings, we measured the intracellular concentration of SN-38 in treated cells. Higher SN-38 concentrations were found in endothelial cells exposed to the combined schedule if compared with treatment using single drug alone, as demonstrated by the area under the peak of the chromatograms (Figure 5, *A-E*). Figure 5*F* quantified the significant increase of intracellular SN-38 concentration normalized to 10^5 cells.

SN-38 and Axitinib Combination Increased the Secretion of TSP-1 in Conditioned Media and Decreased VEGFR-2 in HMVEC-d Cells

The exposure of endothelial cells to axitinib and SN-38 for 72 hours at concentrations that determined a 50% inhibition of cell proliferation determined a significant increase of TSP-1 secretion in the medium and a decrease in VEGF secretion (Figure 6*A*). Of note, the same percentage of TSP-1 increase was obtained by the simultaneous exposure to axitinib and SN-38 at much lower concentrations.

Moreover, the drug combination significantly decreased the VEGFR-2 protein level in endothelial cell lysates in a concentration-dependent manner (Figure 6*B*), even at very low concentrations.

Axitinib Improves the Antitumor Activity of Irinotecan In Vivo

Capan-1 cells injected subcutaneously (s.c.) in CD *nu/nu* mice grew quite rapidly, and tumor masses became detectable 8 to 10 days after xenotransplantation. Tumors in control animals showed a exponential enlargement in their dimensions. Both axitinib and CPT-11, alone and in combination, were able to inhibit tumor growth, although to different extents (Figures 7 and W1*A*). During the 31 days of treatment, axitinib was significantly effective at inhibiting tumor growth (e.g., at day 31, 136.8 *vs* 1389 mm^3 of controls, $P < .05$) and greater than CPT-11 (476.2 mm^3). In the group of animals receiving the combined treatment of axitinib and CPT-11, regression of tumors was almost complete (e.g., at day 31, 67.9 mm^3), and it was always significant when compared to CPT-11 and on days 14 and 17 also when compared to axitinib (Figures 7 and W1*B*). The toxicity profile was favorable for axitinib, with no loss of weight throughout the course of the experiment (Figure W2). As expected, the mice treated with CPT-11 showed a 15% of weight loss compared with controls, whereas the combination treatment caused a maximum weight loss of 30% (Figure W2). Mouse weights successfully recovered with simple veterinary assistance consisting in a fluid therapy (0.9% saline, 40-80 ml/kg s.c. every 24 hours) as recommended by the academic committee for the animal experimentation and by the guidelines of animals in cancer research [32]. No toxic deaths occurred.

The subcutaneous injection of Capan-1 pancreatic cancer cells caused tumors, the histologic picture of which was consistent with pancreatic cancer. As shown in Figure 8*A*, treatment using the simultaneous combination of axitinib and CPT-11 significantly reduced the microvessel count in the tumor mass when compared to controls. Panels *B* and *C* of Figure 8 are representative microscopic pictures of the quantified reduction of microvessels in the control and treated tumors with the combination schedule.

As shown in Figure 8*D*, tumors administered with the combination treatment determined a significant increase in tumor apoptosis

as demonstrated by increased activated caspase-3 staining of paraffin-embedded specimens, if compared to controls and single drugs alone. Panels *E* and *F* of Figure 8 are representative microscopic pictures of the quantified increase of caspase-3 staining in the control and treated tumors with the combination schedule.

Discussion

There is an increasing interest in the clinical development of axitinib, an oral inhibitor of VEGF receptors-1, -2, and -3 having proven anti-angiogenic effect [4]. Indeed, the drug has demonstrated a wide range of activity against various tumors in phase 2 studies, including thyroid cancer [33], advanced non–small cell lung cancer, and metastatic renal cell carcinoma [34,35], as well as pancreatic cancer in combination with gemcitabine [1]. Recently, original combinations of chemotherapeutic schedules were reported in the context of a phase 1 study on metastatic colorectal cancer and other solid tumors, including axitinib in combination with FOLFIRI (irinotecan, 5-fluorouracil, leucovorin), or FOLFOX (oxaliplatin, 5-fluorouracil, leucovorin) and with or without bevacizumab [36]. In fact, axitinib, given at a starting dosage of 5 mg twice a day, was well tolerated in combination with FOLFOX or FOLFIRI, with no dose-limiting toxicities observed [36]. Moreover, this combination is currently being tested in an ongoing, open-label, randomized, multicenter phase 2 clinical trial (NCT00615056), illustrating the clinical interest in assessing axitinib with schedules containing irinotecan.

Our study clearly demonstrated, for the first time, that the axitinib and irinotecan combination was highly synergistic *in vitro*, targeting both endothelial and pancreas cancer cells. This is of considerable interest not only for the ongoing colorectal cancer trials but also for planning new pancreas cancer treatments in the future. In this regard, this tumor type has clinically been shown to have a significant inherent resistance to chemotherapeutic drugs and anti-VEGF treatments [37]; thus, a novel synergistic approach is urgently needed based on novel mechanism of actions. The previous preclinical data are almost all related to the *in vivo* inhibition of tumor growth and angiogenesis by axitinib [4,6,10], and no data are available on the extent of antiproliferative and proapoptotic effect *in vitro* both alone or in combination with chemotherapeutic drugs on proliferating endothelial and

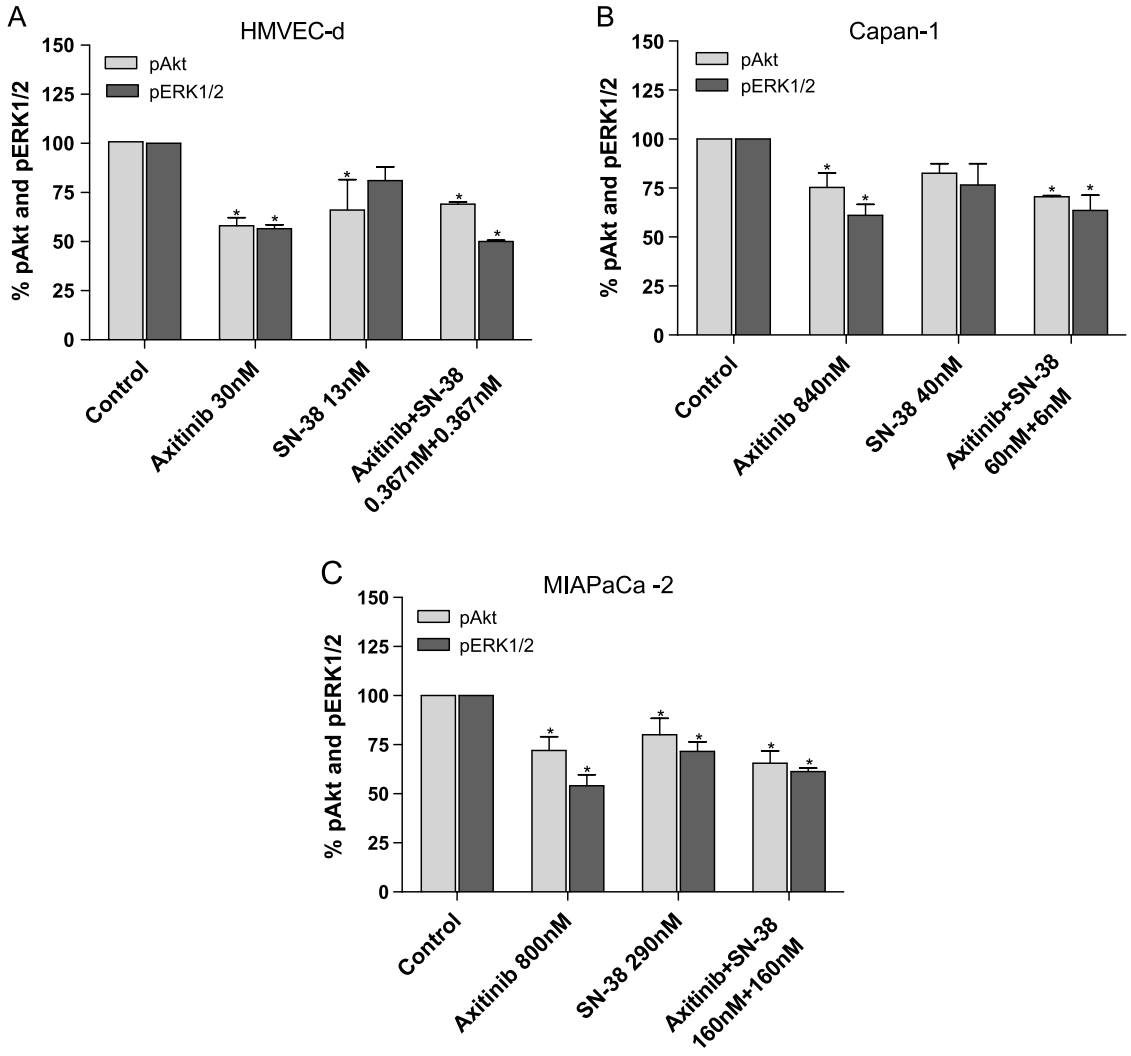

Figure 3. Modulation of Akt (pThr^{308}) and ERK1/2 (pThr^{185}/pTyr^{187}) phosphorylation by axitinib, SN-38, and their combination in HMVEC-d (A), Capan-1 (B), and MIAPaCa-2 (C) cells after 72 hours of treatment. pAkt and pERK1/2 concentrations were measured by ELISA kits, and they were normalized to total Akt and ERK1/2 protein concentration, respectively. Columns and bars indicate mean values ± SE, respectively. *$P < .05$ *versus* vehicle-treated controls.

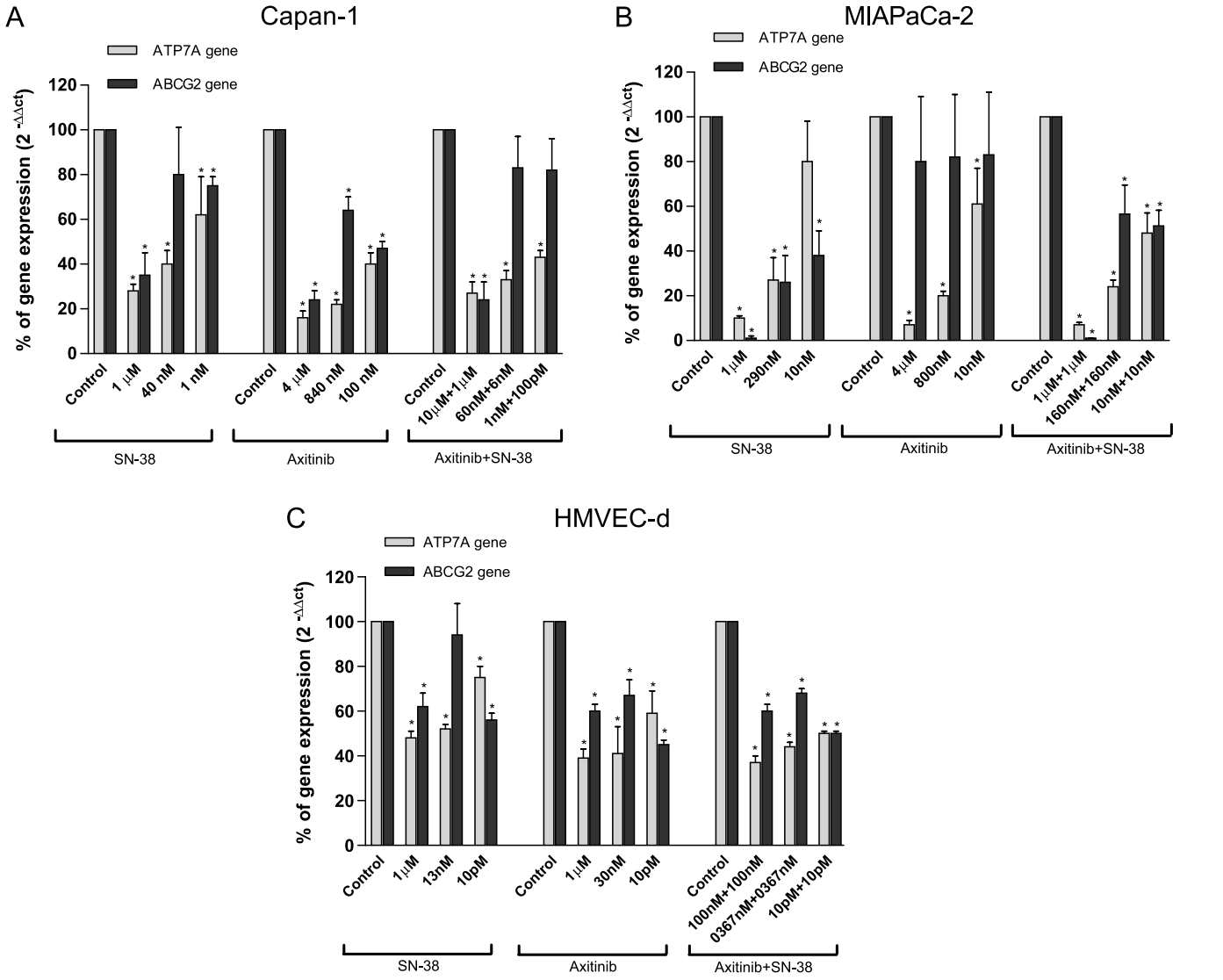

Figure 4. *ATP7A* and *ABCG2* gene expression in Capan-1 (A), MIAPaCa-2 (B), and HMVEC-d (C) cells exposed to axitinib, SN-38, the simultaneous combination of axitinib and SN-38, or with vehicle alone for 72 hours. Columns and bars indicate mean values ± SE, respectively. *$P < .05$ *versus* vehicle-treated controls.

cancer cells. Interestingly, here we show that the antiproliferative and proapoptotic effects are also significant when tested on cancer cells (albeit at higher concentrations compared to endothelial) by axitinib alone, probably related to the inhibition of different tyrosine kinases (e.g., FGFR-1, platelet-derived growth factor receptor) and protein kinases such as Abl and Aurora-2 as demonstrated by Hu-Lowe et al. [4] and by the synergistic action of the simultaneous combination with SN-38. Axitinib has been shown to inhibit *in vitro* both ERK1/2 and Akt phosphorylation in human umbilical vascular endothelial cells and ERK1/2 phosphorylation in tumor samples [4]. Our findings confirm these data in endothelial cells and suggest that cancer cells could be directly affected in the proliferation/apoptosis rate by axitinib through the ERK1/2 and Akt phosphorylation inhibition. Moreover, these effects are amplified by the simultaneous combination of SN-38 and axitinib at much lower concentrations than the single drugs alone, both in endothelial and cancer cells, indicating that it is possible to obtain the same intracellular signal transduction inhibition by markedly reducing the doses of both drugs, as also clearly suggested by the experimental DRIs.

The basis of the significant synergistic activity of the SN-38/irinotecan plus axitinib combination may be the increase of intracellular SN-38 concentration observed after the simultaneous exposure to the two drugs. The inhibition of the gene expression of two relevant transporters of SN-38 such as *ATP7A* and *ABCG2*, both involved in the resistance to irinotecan and other chemotherapeutic drugs [23,26,38], by the simultaneous combination of the drugs, sheds light on the possible mechanism by which the intracellular levels of the active metabolite of irinotecan are significantly increased. Indeed, there is an increasing evidence regarding the capacity to directly inhibit ABC transporters P-glycoprotein by similar drugs such as sunitinib [39,40] or to reduce ABCG2 surface expression in cancer cells by other tyrosine kinase inhibitors like imatinib, nilotinib, and dasatinib [41]. Thus, it is conceivable that the simultaneous administration of axitinib and SN-38 can inhibit expression of ATP7A and ABCG2 at both the mRNA or the protein levels and their functional activity.

Another interesting finding of our study concerns the significant decrease, in a concentration-dependent manner, of VEGFR-2 protein in endothelial cell lysates after the administration of the combination

treatment. This finding could explain the necessity of lower doses of the VEGFR-2 inhibitor drug to maintain a similar inhibition of intracellular signal transduction and the same effects on blocking cell proliferation and promoting the apoptosis process. Moreover, a report by Lee et al. [42] showed that intracellular autonomous VEGF/VEGFR-2 signaling had an indispensable role in vascular homeostasis and endothelial cell survival and that intracellular VEGFR-2 activation in endothelial cells was suppressed by a small-molecule VEGFR antagonist. Thus, it is possible that the drug combination may potently decrease both transmembrane and intracellular VEGFR-2 protein, maintaining even at lower doses the inhibition of VEGFR-2 phosphorylation and autophosphorylation mediated by exogenous VEGF in endothelial cells [42] that ultimately induce endothelial cell apoptosis. Furthermore, numerous studies have reported a significant decrease of plasma soluble VEGFR-2 during and after treatment with VEGFR-2 tyrosine kinase inhibitors such as sunitinib and sorafenib, both in treated animals [43] and in patients [44–47], suggesting a possible use of this receptor as a biomarker of these inhibitors. Recently, Mukohara et al. [48] described in a phase 1 clinical study the significant decrease of sVEGFR-2 by axitinib in Japanese patients, with a significant correlation between these changes and the area under the curve of the drug ($P < .0001$). In this regard, our *in vitro* findings could represent a possible explanation of these previously reported clinical data.

It is noteworthy that the increase of TSP-1, an endogenous inhibitor of angiogenesis, and a decrease of VEGF secretion in the conditioned media of endothelial cells at effective concentrations of the two combined drugs may be additional mechanisms to explain the efficacy of the drug combination. Our group has previously observed that SN-38 caused a significant increase of TSP-1 in conditioned medium of microvascular endothelial cells after 72 hours of treatment [28]. This enhancement of TSP-1 was maintained and even increased in the combined treatment but at lower doses. This observations may be mechanistically linked to the inhibition of Akt phosphorylation as demonstrated by Bussolati et al. [49], who described the modulatory

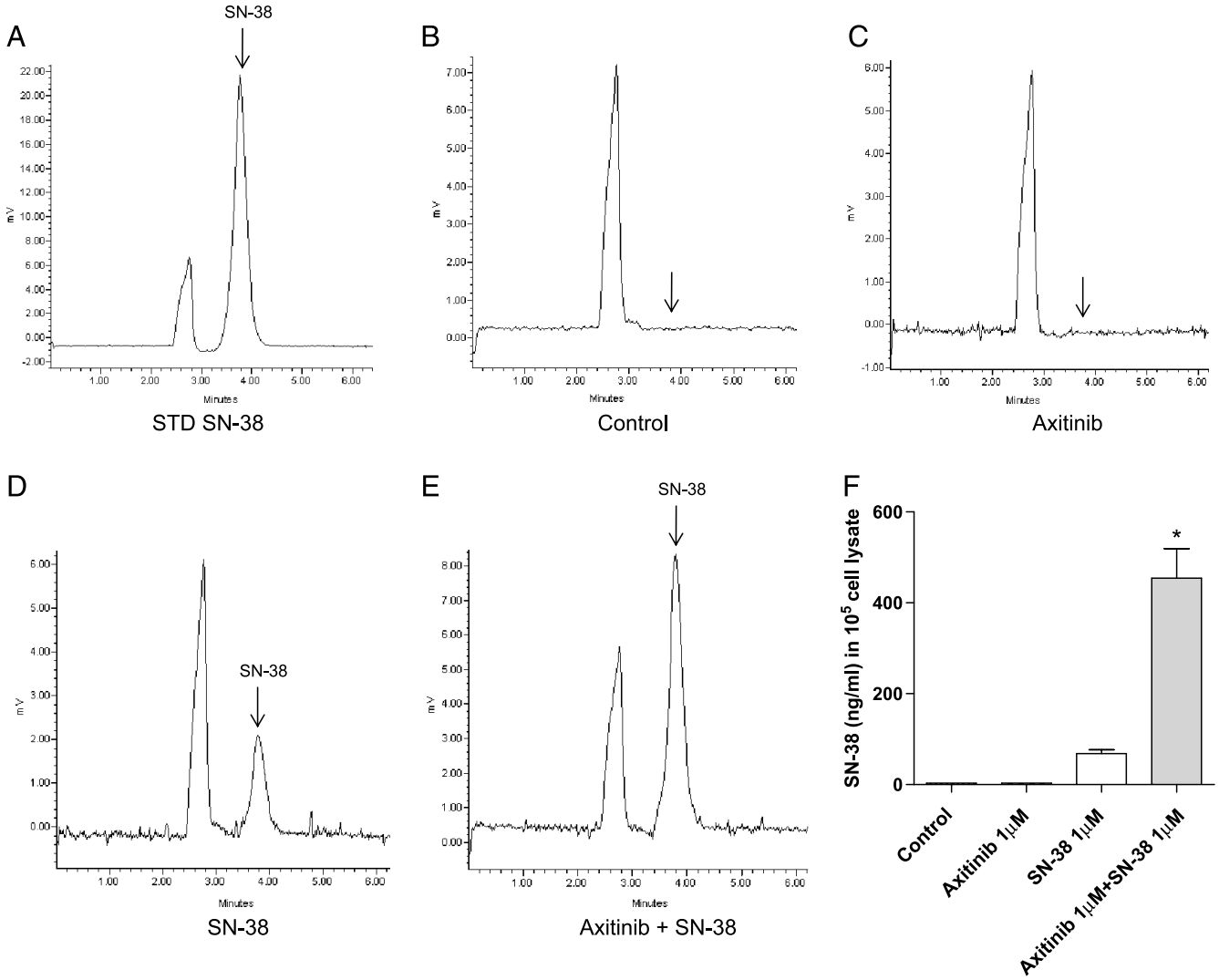

Figure 5. Intracellular SN-38 concentration measurement in HMVEC-d cells after the exposure to axitinib, SN-38, and their simultaneous combination for 72 hours. Representative high-performance liquid chromatography chromatograms of a spiked standard of SN-38 (A), drug-free vehicle-treated sample (blank, B), axitinib-treated sample (C), SN-38-treated sample (D), and axitinib + SN-38 combination sample (E). Interfering peaks were not noted at the retention time of SN-38 (arrow) in the drug-free sample. Quantification of the SN-38 concentrations in 10^5 HMVEC-d cells (F). Columns and bars indicate mean values ± SE, respectively. *$P < .05$ *versus* SN-38–treated samples.

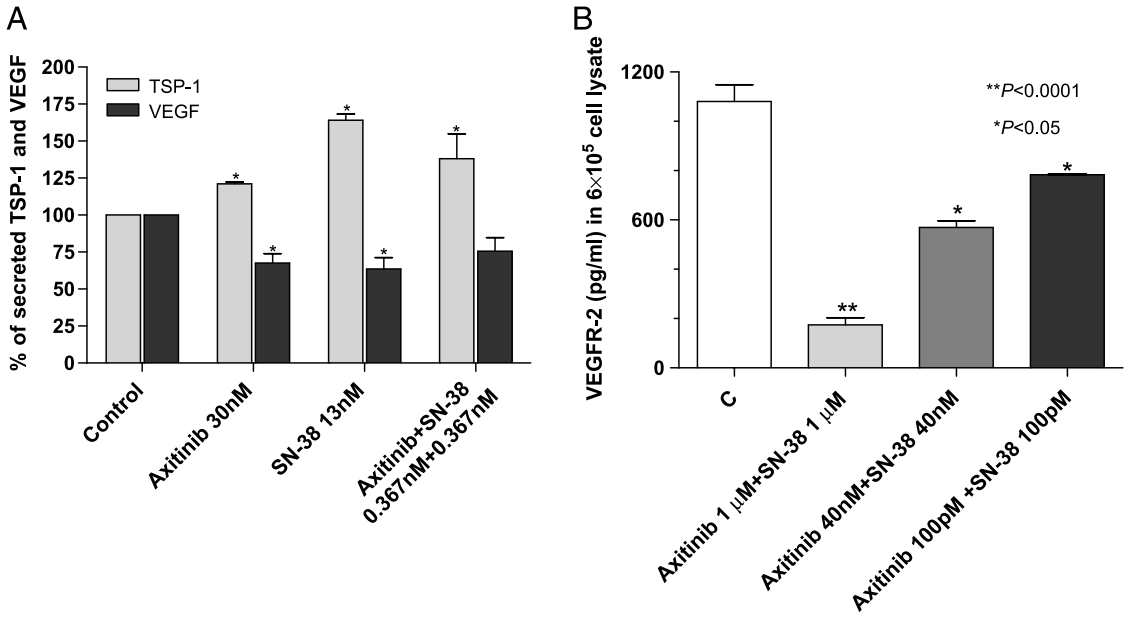

Figure 6. TSP-1 and VEGF secretion (A) in the conditioned media of HMVEC-d cells exposed to axitinib, SN-38, and their simultaneous combination or with vehicle alone for 72 hours. Columns and bars indicate mean values ± SE, respectively. *$P < .05$ *versus* vehicle-treated controls. TSP-1 and VEGF concentrations in conditioned media were measured with ELISA kit and normalized to total protein concentration. VEGFR-2 concentration (B) in 6×10^5 HMVEC-d cell lysate after the exposure to axitinib, SN-38, and their simultaneous combination or with vehicle alone for 72 hours. Columns and bars indicate mean values ± SE, respectively. *$P < .05$, **$P < .001$ *versus* vehicle-treated controls.

role of Akt on TSP-1 synthesis in tumor endothelial cells. Indeed, the inhibition of Akt activation by administration of PI3K inhibitors significantly stimulated the synthesis and release of TSP-1 in tumor endothelial cell [49], in agreement with previous data by Niu et al. [50], who have shown that a loss of Akt signaling was related to a gradual increase in TSP-1 levels in endothelial cells.

To proceed with the development of the concurrent combination of CPT-11 and axitinib, the second step was to evaluate the antitumor and antiangiogenic activity of this schedule *in vivo*. On the basis of our previous experience [28] and from data of previously published studies [4], we decided to treat animals with an maximum tolerated dose (MTD) CPT-11 regimen (100 mg/kg weekly), an optimal dose axitinib schedule (25 mg/kg p.o. twice/day), and with the simultaneous combination of this two regimens. The axitinib schedule was very well tolerated, as expected from the published experience in other tumor models [4], when compared with the CPT-11 MTD regimen. Moreover, the results suggested an improved efficacy of the combined regimen (at least for some time points), with a significant but still acceptable toxicity profile if a simple veterinary assistance (saline injections) was provided; this enhanced activity was due to the combination of a direct effect of irinotecan MTD dose on both drug-sensitive tumor cells and proliferating endothelial cells [51,52] and to a prolonged antitumor and antiangiogenic effect *in vivo* of axitinib [4]. Indeed, the continuous administration of the

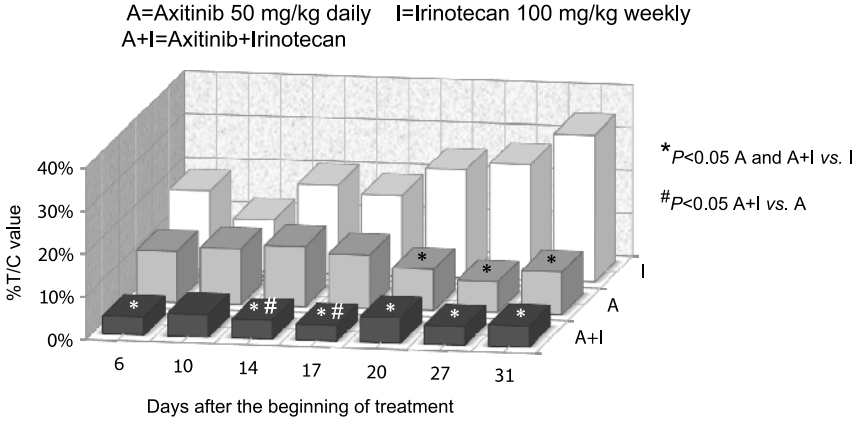

Figure 7. *In vivo* antitumor effects of the single drugs (irinotecan 100 mg/kg i.p. every week and axitinib 25 mg/kg p.o. twice/daily) and simultaneous combination of irinotecan and axitinib schedules on Capan-1 tumors xenotransplanted in CD *nu/nu* mice expressed as percent *T/C* value. Columns indicate percent T/C values. *$P < .05$ axitinib alone and axitinib + irinotecan *versus* irinotecan alone; #$P < .05$ axitinib + irinotecan *versus* axitinib alone. A indicates axitinib; A + I, axitinib + irinotecan; I, irinotecan.

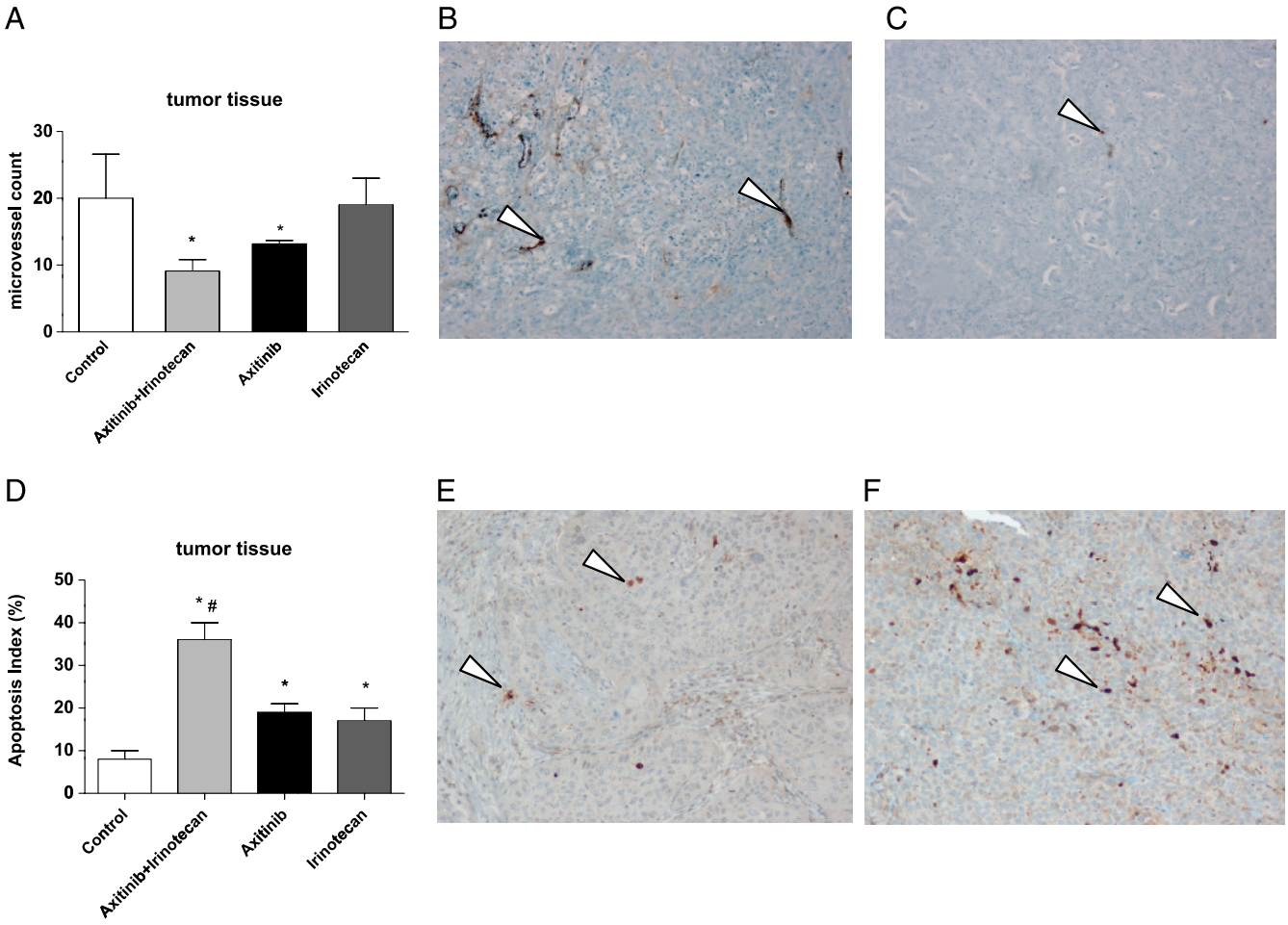

Figure 8. Quantification of microvessel density in Capan-1 tumor xenografts administered with vehicle, irinotecan 100 mg/kg i.p. every week, axitinib 25 mg/kg p.o. twice/daily, and their simultaneous combination schedule at the end of 31 days of treatments (A). Columns and bars indicate mean values ± SE, respectively. *$P < .05$ *versus* vehicle-treated controls. Representative images of IHC of mouse FVIII in Capan-1 xenografts in vehicle-treated mice (control group) (B) and in irinotecan 100 mg/kg i.p. every week + axitinib 25 mg/kg p.o. twice/daily group of mice (C). Quantification of tumor apoptosis as detected by caspase-3 staining (D). Columns and bars indicate mean values ± SE, respectively. *$P < .05$ *versus* vehicle-treated controls; $^{\#}P < .05$ *versus* axitinib- and irinotecan-treated alone groups. Representative images of IHC of active caspase-3 in Capan-1 xenografts in vehicle-treated mice (control group) (E) and in irinotecan 100 mg/kg i.p. every week + axitinib 25 mg/kg p.o. twice/daily group of mice (F). Arrowheads indicate positively stained cells. Magnification, ×200.

VEGFR-2 tyrosine kinase inhibitor alone or in combination with CPT-11 without any breaks was extremely important because it caused an almost complete tumor regression, avoiding the observed rapid tumor (re)growth seen after cessation of therapy with tyrosine kinase inhibitors [43,53].

No preclinical data are currently available on the irinotecan and axitinib combination; however, a phase 1 study of axitinib and irinotecan, but combined with 5-fluorouracil and leucovorin, in patients with advanced colorectal cancer has been recently published, describing an acceptable toxicity profile [36]. Our data experimentally support the preclinical advantage of the association between the continuously administered axitinib and MTD CPT-11 in pancreas cancer and may rapidly improve the possibility to translate this combination therapy into the clinic on a solid basis to enhance the antitumor effects and reduce toxicity. Indeed, our data clearly suggest the possibility to reduce the doses of both drugs, maintaining the same antiangiogenic and antitumor effects.

In conclusion, the clinical development of a promising irinotecan/axitinib schedule and of related pharmacodynamic mechanisms, appears possible. The significance of our results is the development of a rational and less empirical strategy for irinotecan/axitinib combination "from bench to bedside". Indeed, our study focuses on possible new approaches with respect to addressing the major questions regarding the clinical application of combined schedules between chemotherapeutic drugs and VEGFRs inhibitors that relate to the actual antitumor/antiangiogenic activity of the chosen combination, the dosing levels, the frequency of administration, the possible pharmacodynamic surrogate markers to be used to monitor the therapy (e.g., *ATP7A* and *ABCG2* gene expression, VEGFR-2 and TSP-1 protein concentration). Indeed, based on our experimental data, we could suggest initiating pilot phase 2 clinical trials with at least the following characteristics: 1) a simultaneous combination of irinotecan and daily axitinib without any breaks in pancreas cancer patients (including patients whose tumors are already resistant to irinotecan, but who may respond again because of the inhibition of ATP7A and ABCG2 transporters), 2) the irinotecan and axitinib dose levels being reduced with respect to their maximum tolerated total dose or optimal biologic dose, and 3) the antitumor/antiangiogenic activity assessed with pharmacodynamic parameters

such as, for example, *ATP7A* and *ABCG2* gene expression in peripheral blood mononuclear cell, or VEGFR-2 and TSP-1 plasma levels.

Acknowledgments

The authors thank Franco Bocci.

References

[1] Spano JP, Chodkiewicz C, Maurel J, Wong R, Wasan H, Barone C, Letourneau R, Bajetta E, Pithavala Y, Bycott P, et al. (2008). Efficacy of gemcitabine plus axitinib compared with gemcitabine alone in patients with advanced pancreatic cancer: an open-label randomised phase II study. *Lancet* **371**, 2101–2108.

[2] Kelly RJ and Rixe O (2009). Axitinib—a selective inhibitor of the vascular endothelial growth factor (VEGF) receptor. *Target Oncol* **4**, 297–305.

[3] Solowiej J, Bergqvist S, McTigue MA, Marrone T, Quenzer T, Cobbs M, Ryan K, Kania RS, Diehl W, and Murray BW (2009). Characterizing the effects of the juxtamembrane domain on vascular endothelial growth factor receptor-2 enzymatic activity, autophosphorylation, and inhibition by axitinib. *Biochemistry* **48**, 7019–7031.

[4] Hu-Lowe DD, Zou HY, Grazzini ML, Hallin ME, Wickman GR, Amundson K, Chen JH, Rewolinski DA, Yamazaki S, Wu EY, et al. (2008). Nonclinical antiangiogenesis and antitumor activities of axitinib (AG-013736), an oral, potent, and selective inhibitor of vascular endothelial growth factor receptor tyrosine kinases 1, 2, 3. *Clin Cancer Res* **14**, 7272–7283.

[5] Wilmes LJ, Pallavicini MG, Fleming LM, Gibbs J, Wang D, Li KL, Partridge SC, Henry RG, Shalinsky DR, Hu-Lowe D, et al. (2007). AG-013736, a novel inhibitor of VEGF receptor tyrosine kinases, inhibits breast cancer growth and decreases vascular permeability as detected by dynamic contrast-enhanced magnetic resonance imaging. *Magn Reson Imaging* **25**, 319–327.

[6] Ma J and Waxman DJ (2009). Dominant effect of antiangiogenesis in combination therapy involving cyclophosphamide and axitinib. *Clin Cancer Res* **15**, 578–588.

[7] Fenton BM and Paoni SF (2007). The addition of AG-013736 to fractionated radiation improves tumor response without functionally normalizing the tumor vasculature. *Cancer Res* **67**, 9921–9928.

[8] Fenton BM and Paoni SF (2009). Alterations in daily sequencing of axitinib and fractionated radiotherapy do not affect tumor growth inhibition or pathophysiological response. *Radiat Res* **171**, 606–614.

[9] Nakahara T, Norberg SM, Shalinsky DR, Hu-Lowe DD, and McDonald DM (2006). Effect of inhibition of vascular endothelial growth factor signaling on distribution of extravasated antibodies in tumors. *Cancer Res* **66**, 1434–1445.

[10] Ma J and Waxman DJ (2008). Modulation of the antitumor activity of metronomic cyclophosphamide by the angiogenesis inhibitor axitinib. *Mol Cancer Ther* **7**, 79–89.

[11] O'Reilly EM (2009). Pancreatic adenocarcinoma: new strategies for success. *Gastrointest Cancer Res* **3**, S11–S15.

[12] Bocci G, Fioravanti A, Orlandi P, Bernardini N, Collecchi P, Del Tacca M, and Danesi R (2005). Fluvastatin synergistically enhances the antiproliferative effect of gemcitabine in human pancreatic cancer MIAPaCa-2 cells. *Br J Cancer* **93**, 319–330.

[13] Bocci G, Danesi R, Marangoni G, Fioravanti A, Boggi U, Esposito I, Fasciani A, Boschi E, Campani D, Bevilacqua G, et al. (2004). Antiangiogenic versus cytotoxic therapeutic approaches to human pancreas cancer: an experimental study with a vascular endothelial growth factor receptor-2 tyrosine kinase inhibitor and gemcitabine. *Eur J Pharmacol* **498**, 9–18.

[14] Bruns CJ, Shinohara H, Harbison MT, Davis DW, Nelkin G, Killion JJ, McConkey DJ, Dong Z, and Fidler IJ (2000). Therapy of human pancreatic carcinoma implants by irinotecan and the oral immunomodulator JBT 3002 is associated with enhanced expression of inducible nitric oxide synthase in tumor-infiltrating macrophages. *Cancer Res* **60**, 2–7.

[15] Dineen SP, Sullivan LA, Beck AW, Miller AF, Carbon JG, Mamluk R, Wong H, and Brekken RA (2008). The Adnectin CT-322 is a novel VEGF receptor 2 inhibitor that decreases tumor burden in an orthotopic mouse model of pancreatic cancer. *BMC Cancer* **8**, 352.

[16] Mishra G, Butler J, Ho C, Melin S, Case LD, Ennever PR, Magrinat GC, Bearden JD, Minotto DC, Howerton R, et al. (2005). Phase II trial of induction gemcitabine/CPT-11 followed by a twice-weekly infusion of gemcitabine and concurrent external beam radiation for the treatment of locally advanced pancreatic cancer. *Am J Clin Oncol* **28**, 345–350.

[17] Rocha Lima CM, Sherman CA, Brescia FJ, Brunson CY, and Green MR (2001). Irinotecan/gemcitabine combination chemotherapy in pancreatic cancer. *Oncology (Williston Park)* **15**, 46–51.

[18] Bissery MC, Vrignaud P, Lavelle F, and Chabot GG (1996). Experimental antitumor activity and pharmacokinetics of the camptothecin analog irinotecan (CPT-11) in mice. *Anticancer Drugs* **7**, 437–460.

[19] Rosen LS (1998). Irinotecan in lymphoma, leukemia, and breast, pancreatic, ovarian, and small-cell lung cancers. *Oncology (Williston Park)* **12**, 103–109.

[20] Agrawal S, Kandimalla ER, Yu D, Ball R, Lombardi G, Lucas T, Dexter DL, Hollister BA, and Chen SF (2002). GEM 231, a second-generation antisense agent complementary to protein kinase A RIα subunit, potentiates antitumor activity of irinotecan in human colon, pancreas, prostate and lung cancer xenografts. *Int J Oncol* **21**, 65–72.

[21] DeRosier LC, Buchsbaum DJ, Oliver PG, Huang ZQ, Sellers JC, Grizzle WE, Wang W, Zhou T, Zinn KR, Long JW, et al. (2007). Combination treatment with TRA-8 anti death receptor 5 antibody and CPT-11 induces tumor regression in an orthotopic model of pancreatic cancer. *Clin Cancer Res* **13**, 5535s–5543s.

[22] Kusuhara H and Sugiyama Y (2007). ATP-binding cassette, subfamily G (ABCG family). *Pflugers Arch* **453**, 735–744.

[23] Candeil L, Gourdier I, Peyron D, Vezzio N, Copois V, Bibeau F, Orsetti B, Scheffer GL, Ychou M, Khan QA, et al. (2004). ABCG2 overexpression in colon cancer cells resistant to SN38 and in irinotecan-treated metastases. *Int J Cancer* **109**, 848–854.

[24] Takara K, Kitada N, Yoshikawa E, Yamamoto K, Horibe S, Sakaeda T, Nishiguchi K, Ohnishi N, and Yokoyama T (2009). Molecular changes to HeLa cells on continuous exposure to SN-38, an active metabolite of irinotecan hydrochloride. *Cancer Lett* **278**, 88–96.

[25] Furukawa T, Komatsu M, Ikeda R, Tsujikawa K, and Akiyama S (2008). Copper transport systems are involved in multidrug resistance and drug transport. *Curr Med Chem* **15**, 3268–3278.

[26] Owatari S, Akune S, Komatsu M, Ikeda R, Firth SD, Che XF, Yamamoto M, Tsujikawa K, Kitazono M, Ishizawa T, et al. (2007). Copper-transporting P-type ATPase, ATP7A, confers multidrug resistance and its expression is related to resistance to SN-38 in clinical colon cancer. *Cancer Res* **67**, 4860–4868.

[27] Chou TC (2006). Theoretical basis, experimental design, and computerized simulation of synergism and antagonism in drug combination studies. *Pharmacol Rev* **58**, 621–681.

[28] Bocci G, Falcone A, Fioravanti A, Orlandi P, Di Paolo A, Fanelli G, Viacava P, Naccarato AG, Kerbel RS, Danesi R, et al. (2008). Antiangiogenic and anticolorectal cancer effects of metronomic irinotecan chemotherapy alone and in combination with semaxinib. *Br J Cancer* **98**, 1619–1629.

[29] Allegrini G, Falcone A, Fioravanti A, Barletta MT, Orlandi P, Loupakis F, Cerri E, Masi G, Di Paolo A, Kerbel RS, et al. (2008). A pharmacokinetic and pharmacodynamic study on metronomic irinotecan in metastatic colorectal cancer patients. *Br J Cancer* **98**, 1312–1319.

[30] Simon PO Jr, McDunn JE, Kashiwagi H, Chang K, Goedegebuure PS, Hotchkiss RS, and Hawkins WG (2009). Targeting AKT with the proapoptotic peptide, TAT-CTMP: a novel strategy for the treatment of human pancreatic adenocarcinoma. *Int J Cancer* **125**, 942–951.

[31] Bressenot A, Marchal S, Bezdetnaya L, Garrier J, Guillemin F, and Plenat F (2009). Assessment of apoptosis by immunohistochemistry to active caspase-3, active caspase-7, or cleaved PARP in monolayer cells and spheroid and subcutaneous xenografts of human carcinoma. *J Histochem Cytochem* **57**, 289–300.

[32] Workman P, Aboagye EO, Balkwill F, Balmain A, Bruder G, Chaplin DJ, Double JA, Everitt J, Farningham DA, Glennie MJ, et al. (2010). Guidelines for the welfare and use of animals in cancer research. *Br J Cancer* **102**, 1555–1577.

[33] Cohen EE, Rosen LS, Vokes EE, Kies MS, Forastiere AA, Worden FP, Kane MA, Sherman E, Kim S, Bycott P, et al. (2008). Axitinib is an active treatment for all histologic subtypes of advanced thyroid cancer: results from a phase II study. *J Clin Oncol* **26**, 4708–4713.

[34] Schiller JH, Larson T, Ou SH, Limentani S, Sandler A, Vokes E, Kim S, Liau K, Bycott P, Olszanski AJ, et al. (2009). Efficacy and safety of axitinib in patients with advanced non–small-cell lung cancer: results from a phase II study. *J Clin Oncol* **27**, 3836–3841.

[35] Rini BI, Wilding G, Hudes G, Stadler WM, Kim S, Tarazi J, Rosbrook B, Trask PC, Wood L, and Dutcher JP (2009). Phase II study of axitinib in sorafenib-refractory metastatic renal cell carcinoma. *J Clin Oncol* **27**, 4462–4468.

[36] Sharma S, Abhyankar V, Burgess RE, Infante J, Trowbridge RC, Tarazi J, Kim S, Tortorici M, Chen Y, and Robles RL (2010). A phase I study of axitinib

(AG-013736) in combination with bevacizumab plus chemotherapy or chemotherapy alone in patients with metastatic colorectal cancer and other solid tumors. *Ann Oncol* **21**, 297–304.

[37] Ferrara N (2010). Pathways mediating VEGF-independent tumor angiogenesis. *Cytokine Growth Factor Rev* **21**, 21–26.

[38] Bates SE, Medina-Perez WY, Kohlhagen G, Antony S, Nadjem T, Robey RW, and Pommier Y (2004). ABCG2 mediates differential resistance to SN-38 (7-ethyl-10-hydroxycamptothecin) and homocamptothecins. *J Pharmacol Exp Ther* **310**, 836–842.

[39] Dai CL, Liang YJ, Wang YS, Tiwari AK, Yan YY, Wang F, Chen ZS, Tong XZ, and Fu LW (2009). Sensitization of ABCG2-overexpressing cells to conventional chemotherapeutic agent by sunitinib was associated with inhibiting the function of ABCG2. *Cancer Lett* **279**, 74–83.

[40] Shukla S, Robey RW, Bates SE, and Ambudkar SV (2009). Sunitinib (Sutent, SU11248), a small-molecule receptor tyrosine kinase inhibitor, blocks function of the ATP-binding cassette (ABC) transporters P-glycoprotein (ABCB1) and ABCG2. *Drug Metab Dispos* **37**, 359–365.

[41] Dohse M, Scharenberg C, Shukla S, Robey RW, Volkmann T, Deeken JF, Brendel C, Ambudkar SV, Neubauer A, and Bates SE (2010). Comparison of ATP-binding cassette transporter interactions with the tyrosine kinase inhibitors imatinib, nilotinib, and dasatinib. *Drug Metab Dispos* **38**, 1371–1380.

[42] Lee S, Chen TT, Barber CL, Jordan MC, Murdock J, Desai S, Ferrara N, Nagy A, Roos KP, and Iruela-Arispe ML (2007). Autocrine VEGF signaling is required for vascular homeostasis. *Cell* **130**, 691–703.

[43] Ebos JM, Lee CR, Christensen JG, Mutsaers AJ, and Kerbel RS (2007). Multiple circulating proangiogenic factors induced by sunitinib malate are tumor-independent and correlate with antitumor efficacy. *Proc Natl Acad Sci USA* **104**, 17069–17074.

[44] Deprimo SE, Bello CL, Smeraglia J, Baum CM, Spinella D, Rini BI, Michaelson MD, and Motzer RJ (2007). Circulating protein biomarkers of pharmacodynamic activity of sunitinib in patients with metastatic renal cell carcinoma: modulation of VEGF and VEGF-related proteins. *J Transl Med* **5**, 32.

[45] Motzer RJ, Michaelson MD, Redman BG, Hudes GR, Wilding G, Figlin RA, Ginsberg MS, Kim ST, Baum CM, DePrimo SE, et al. (2006). Activity of SU11248, a multitargeted inhibitor of vascular endothelial growth factor receptor and platelet-derived growth factor receptor, in patients with metastatic renal cell carcinoma. *J Clin Oncol* **24**, 16–24.

[46] Pena C, Lathia C, Shan M, Escudier B, and Bukowski RM (2010). Biomarkers predicting outcome in patients with advanced renal cell carcinoma: results from sorafenib phase III treatment approaches in renal cancer global evaluation trial. *Clin Cancer Res* **16**, 4853–4863.

[47] Norden-Zfoni A, Desai J, Manola J, Beaudry P, Force J, Maki R, Folkman J, Bello C, Baum C, DePrimo SE, et al. (2007). Blood-based biomarkers of SU11248 activity and clinical outcome in patients with metastatic imatinib-resistant gastrointestinal stromal tumor. *Clin Cancer Res* **13**, 2643–2650.

[48] Mukohara T, Nakajima H, Mukai H, Nagai S, Itoh K, Umeyama Y, Hashimoto J, and Minami H (2010). Effect of axitinib (AG-013736) on fatigue, thyroid-stimulating hormone, and biomarkers: a phase I study in Japanese patients. *Cancer Sci* **101**, 963–968.

[49] Bussolati B, Assenzio B, Deregibus MC, and Camussi G (2006). The pro-angiogenic phenotype of human tumor-derived endothelial cells depends on thrombospondin-1 downregulation via phosphatidylinositol 3-kinase/Akt pathway. *J Mol Med* **84**, 852–863.

[50] Niu Q, Perruzzi C, Voskas D, Lawler J, Dumont DJ, and Benjamin LE (2004). Inhibition of Tie-2 signaling induces endothelial cell apoptosis, decreases Akt signaling, and induces endothelial cell expression of the endogenous anti-angiogenic molecule, thrombospondin-1. *Cancer Biol Ther* **3**, 402–405.

[51] Ji Y, Hayashi K, Amoh Y, Tsuji K, Yamauchi K, Yamamoto N, Tsuchiya H, Tomita K, Bouvet M, and Hoffman RM (2007). The camptothecin derivative CPT-11 inhibits angiogenesis in a dual-color imageable orthotopic metastatic nude mouse model of human colon cancer. *Anticancer Res* **27**, 713–718.

[52] Kamiyama H, Takano S, Tsuboi K, and Matsumura A (2005). Anti-angiogenic effects of SN38 (active metabolite of irinotecan): inhibition of hypoxia-inducible factor 1 α (HIF-1α)/vascular endothelial growth factor (VEGF) expression of glioma and growth of endothelial cells. *J Cancer Res Clin Oncol* **131**, 205–213.

[53] Ebos JM, Lee CR, Cruz-Munoz W, Bjarnason GA, Christensen JG, and Kerbel RS (2009). Accelerated metastasis after short-term treatment with a potent inhibitor of tumor angiogenesis. *Cancer Cell* **15**, 232–239.

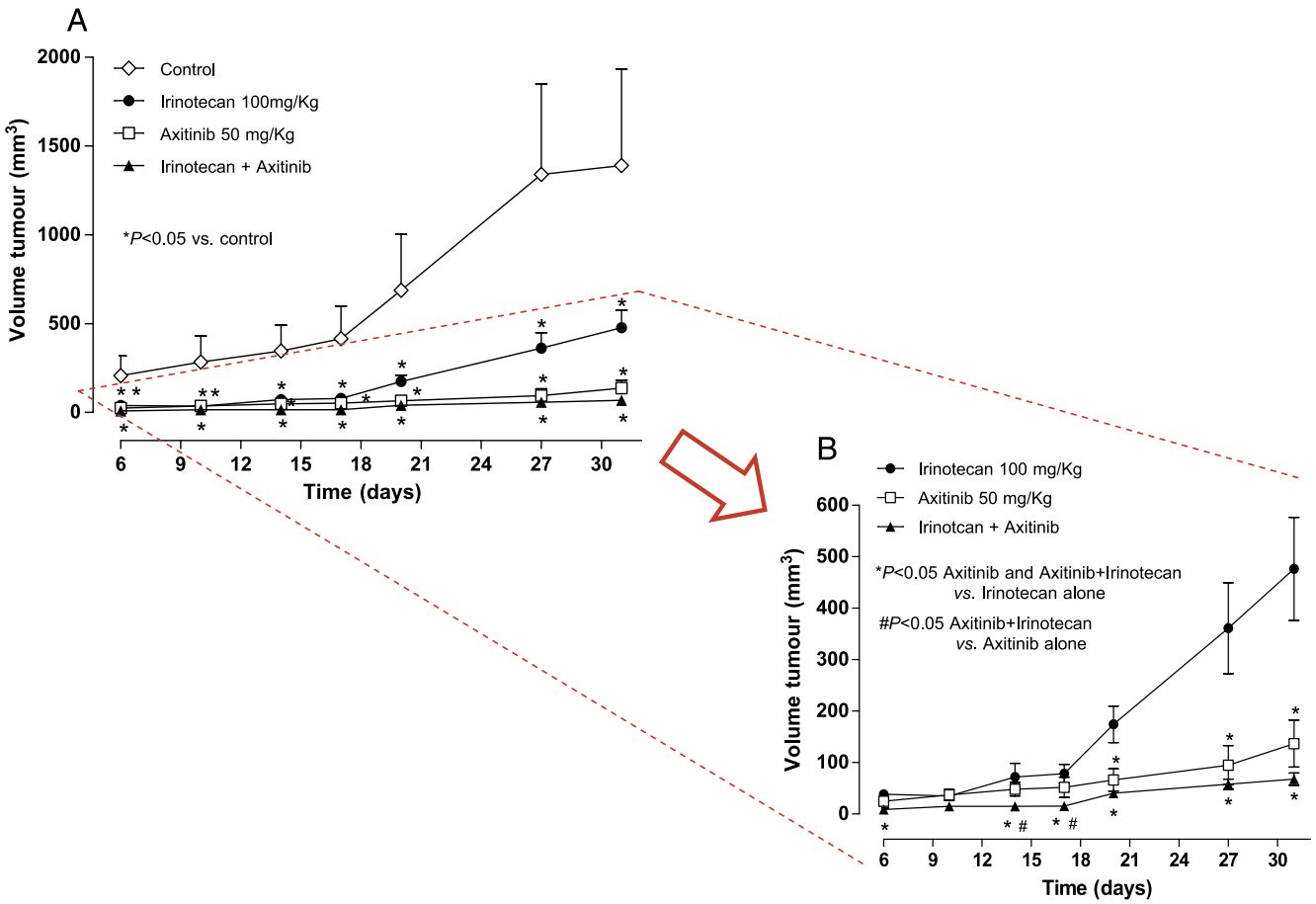

Figure W1. (A) Antitumor effect of 1) irinotecan 100 mg/kg i.p., 2) axitinib 50 mg/kg p.o., and 3) simultaneous combination of irinotecan and axitinib on Capan-1 tumors xenotransplanted in CD *nu/nu* mice. (B) Magnification of both axes for the tumor volume of treated groups only. Symbols and bars indicate mean ± SEM.

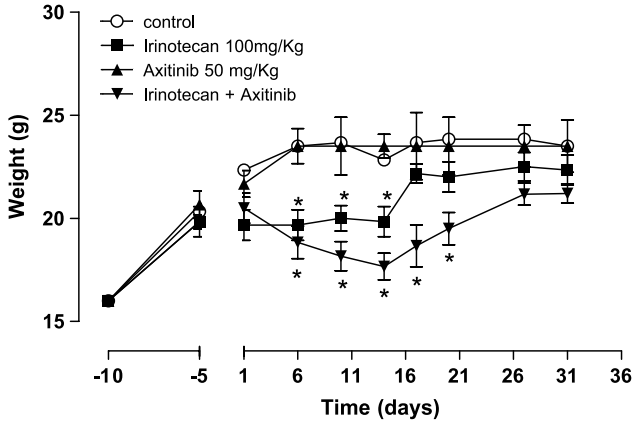

Figure W2. Body weight of Capan-1 tumor-bearing control mice and mice treated with irinotecan, axitinib, and their simultaneous combination. Irinotecan and the irinotecan/axitinib combination caused a loss of weight that required veterinary assistance with a fluid therapy (0.9% saline, 40-80 ml/kg s.c. every 24 hours). Symbols and bars indicate mean ± SEM. $P < .05$ *versus* vehicle-treated controls.